Jordan Journal of Civil Engineering, Volume **14**, No. **2**, **2020**

Bond Behavior of Mortar Anchor under Different Loading Rates

Hai-tao Wang [1)*]***, Zhi-ming Li*** [2)] ***and Hao-yu Sun*** [3)]

[1)] Professor, School of Civil Engineering, Dalian Jiaotong University, Dalian, Liaoning, China.
* Corresponding Author, E-Mail: whtdjtu@163.com
[2)] MSc Student, School of Civil Engineering, Dalian Jiaotong University, Dalian, Liaoning, China.
E-Mail: 396458312@qq.com
[3)] MSc Student, School of Civil Engineering, Dalian Jiaotong University, Dalian, Liaoning, China.
E-Mail: 414861630@qq.com

ABSTRACT

The bond performance of mortar anchor under dynamic load was simulated by dynamic pull-out test of steel bar. The influence of the loading rate, anchoring length and mortar strength on the bond performance was analyzed. The results showed that with the increase of the loading rate, the peak of bond stress increased gradually and the rising part of the bond stress curve changed rapidly. Meanwhile, the strain of the steel along the anchoring depth gradually decreased and the decreasing rate increased gradually. With the increase of the anchoring length, the sum of the bond stress at each point in the anchoring section increased gradually and the bond performance improved. With the increase of the mortar strength, the peak of the bond stress curve moved toward the loading end and the distance transferred by the bond stress along the anchoring depth was small.

KEYWORDS: Strain, Mortar anchor, Bond performance, Anchoring depth, Bond stress.

INTRODUCTION

As a practical reinforcement method used in engineering, geotechnical anchorage technology has become one of the most effective methods to solve the stability problem of geotechnical engineering and is widely used in projects, like foundation pits, roadways, slopes and dams. It has been proved that the anchorage technology is of considerable social and economic value. Except for the low-cost and rapid work progress, the stability of anchoring objects can be effectively improved and the safety and quality of the construction can be ensured with the application of the anchorage technology. With the acceleration of the urbanization process, many large-scale infrastructures have been built in strong earthquake areas and a large number of prestressed anchors in service are used in slope engineering. Therefore, in order to reasonably consider the adverse effects of earthquake action on the anchoring slope engineering (Wang Hai-tao et al., 2019), it is particularly important to study the bond performance of mortar anchor under dynamic load (Ahmet Teymen, 2017; Caliskan, S. et al., 2004; Anwar A. Alnaki et al., 2013).

The bond performance of the anchor rod is mainly determined by the bond between the anchor rod body, the grouting body and the rock-soil body. Scholars have carried out a lot of work to study the load transfer law and the anchoring mechanism of anchor rod under static load (Flavio de Andrade Silva et al., 2011; Gang Wang et al., 2013). Lutz, I. et al. (1967) and Hanson, N.W. et al. (1969) studied the mechanical mechanism of the load transfer from the anchor to the grouting body. They believed that a grouting column was formed around the rough fold of the anchor, where the binding force played a major role before the combination between the anchor and the grout was damaged. The relative displacement between the anchor and the grouting body led to slip failure in a part of the anchor-grout interface, where the frictional resistance played a major role. According to the pull-out test of full-length grouting bolt, Farmer found that when the pull-out load was small, the shear stress of the anchoring section decreased in exponential function curve. When the pull-out load was large, the residual friction stress occurred after the de-bond which

Received on 6/3/2019.
Accepted for Publication on 25/3/2020.

appeared at the loading end. At this period, the anchoring section performed two parts; one was the debonding section distributed horizontally and the other was the elastic-deformation section decrease in exponential function. Based on this, scholars have carried out a series of research studies on the pull-out model of anchor through theoretical analysis, numerical simulation or experimental methods (Tassios, T.P. et al., 1981; Jeng, F.S. et al., 1999).

Compared with the well-established experimental and theoretical studies under static load, the bond performance of steel bars and mortar under dynamic load is less studied. Since the mechanical and deformation properties of steel bars and mortars are different at different loading rates (Pabitra Rajbongshi et al., 2019), the bond performance of mortar anchor under dynamic loading was simulated by the pull-out test of steel bar and mortar at different loading rates (W. Chen et al., 2002; Louis, N.S. et al., 2015). The influence of loading rate, anchoring length and mortar strength on the bond performance was also analyzed (Sreedhar Kalavagunta et al., 2016).

Test Conditions

Test Design

The specimen shape and dimensions shown in Fig. 1 were used in this test. In order to accurately obtain the strain of the steel bar along the anchorage length, reinforced inner patch design was used. After the two ends of the test steel bar are picked out (as shown in Fig. 2 (a)), the steel bar is milled halfway in the axial direction with a wire cutting machine (as shown in Fig. 2 (b) and Fig. 2 (c)) and then along the axis direction on each petal steel bar, a groove is machined (as shown in Fig. 2 (d)), where the size of the groove is 3mm × 4mm (as shown in Fig. 3 (a)). Next, epoxy resin that plays the role of waterproofing, rust prevention and leveling is wiped thinly and uniformly on the surface of the grooves of the reinforcement and a foil-type resistance strain gauge with a size of 2mm × 3mm is pasted in the groove of the reinforcement bonding zone, then resistance strain gauges are attached every 40mm. One piece is arranged staggered up and down (as shown in Fig. 3 (b)) and the gap between the strain gauges after closing is 20mm. After the strain gauges are pasted, white paper is used at the end of the wire and marked to determine the order of the locations of the patches (as shown in Fig. 4 (a)). Then, the wires connecting the strain gauges from both ends of the reinforcing steel are led out (as shown in Fig. 4 (b)). After the wires are led out, the rod is wrapped with a plastic film before grouting to prevent the wires from rusting in a humid environment.

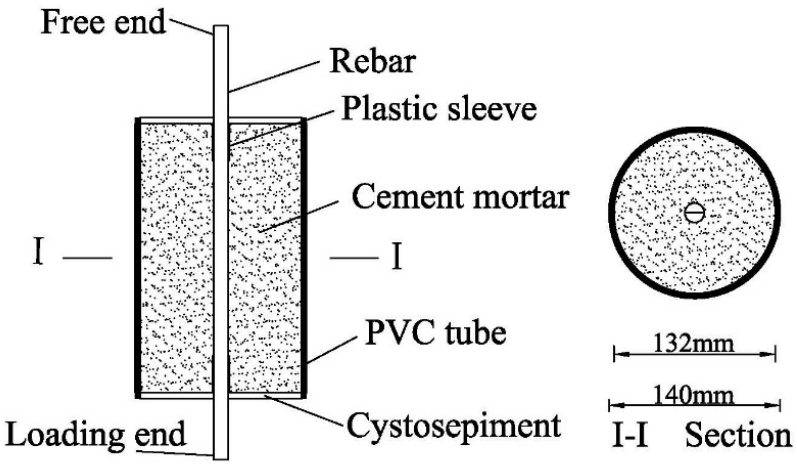

Figure (1): Geometric dimensions of the pull-out specimens used in this study

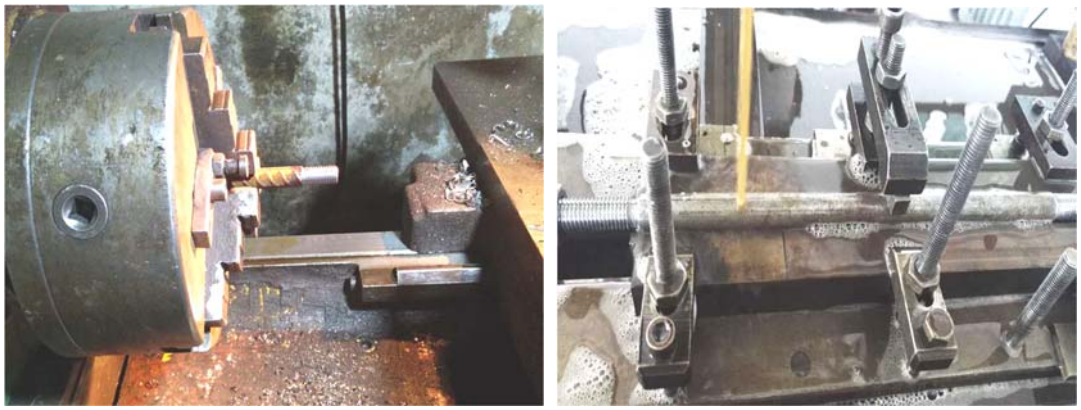

(a) Sketch of pick screw thread (b) Sketch A of cutting by wire cutting machine

(c) Sketch B of cutting by wire cutting machine (d) Sketch of groove machining

Figure (2): Machining processes of steel bars to create grooves where strain gauges are to be installed

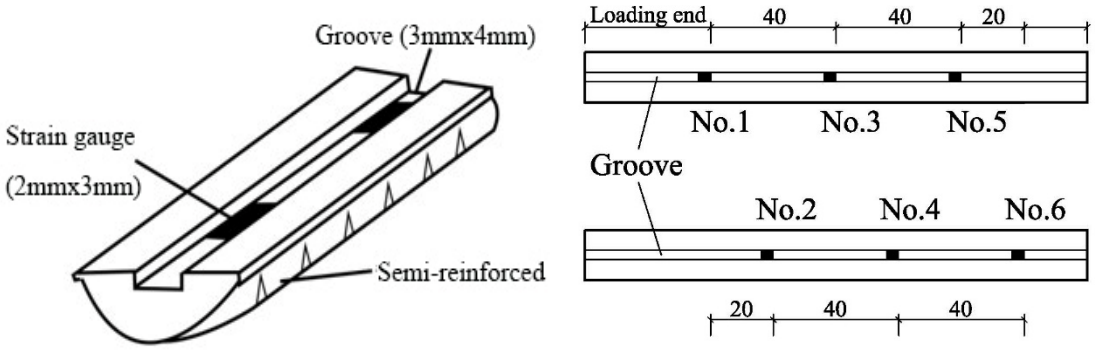

(a) Schematic diagram of grooves and strain gauges (b) Strain gauges layout diagram

Figure (3): Schematics showing strain gauge dimensions and layout diagram within the grooves of the steel bars

(a) Welded halves of steel bars

(b) Sleeves installation on the welded bars

(c) cast pull-out specimens

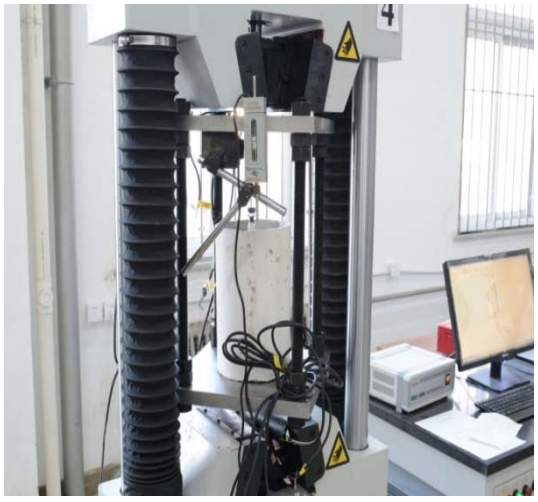

(d) Pull-out specimens mounted on testing machine

Figure (4): Steps of pull-out specimen preparation and testing for bond behavior

Operation occurs according to the requirements of raw materials such as cement mortar for anchor bolts in the Technical Specification for Rock and Soil Bolt Shotcrete Support (GB50086-2015) and the required amount of material is calculated based on the volume of cement mortar to be stirred each time. The electronic scale is accurately weighed and ready for use. The water-reducing agent is dissolved in water and stirred evenly. An appropriate amount of cement mortar is mixed according to the required ratios of water, cement and sand in the mix design and loaded in homemade PVC pipe fittings (as shown in Fig. 4 (c)).

Water-cement ratio, diameter of steel bar, type of steel bar, loading rate and anchoring length were used to study the bond performance of the mortar anchor. The test conditions are shown in Table 1.

It can be observed from Table 2 that the loading rate of 10^{-2}mm/s ~ 1mm/s is static and 1mm/s ~ 10^{2}mm/s is dynamic. The test loading rate is set to 60mm/min (1mm/s), 80mm/min, 100mm/min and 120mm/min (2mm/s).

A 30t electro-hydraulic servo power system was used for displacement control, (as shown in Fig. 4 (d)) and the test loading rates were set to 60mm/min (1mm/s), 80mm/min, 100mm/min and 120mm/min (2mm/s). The specimen was placed in the middle of the loading device, as shown in Fig. 5. The steel bar at one end of the specimen extended along the hole at the loading device and was connected with the grip of the electro-hydraulic servo power system. During the test, the steel bar was pulled out gradually with the operation of the machine. The leads of the strain gauges were connected to a computer dynamic acquisition system to collect the strain data of the steel bar along the anchoring depth.

Table 1. Statistical table of test conditions

Specimen number	Water/ cement ratio	Diameter (mm)	Types of steel bars	Load rate (mm/min)	Anchorage length (mm)	Number of test pieces
MS55G12V12a	0.55	12	Plain bar	120	120	3
MS55G12V10a	0.55	12	Plain bar	100	120	3
MS55G12V10b	0.55	12	Plain bar	100	100	3
MS55G12V12c	0.55	12	Plain bar	120	80	3
MS55G12V12d	0.55	12	Plain bar	120	60	3
MS55G12V10a	0.55	12	Plain bar	100	120	3
MS55G12V8a	0.55	12	Plain bar	80	120	3
MS55G12V6a	0.55	12	Deformed rebar	60	120	3
MS55L12V12a	0.55	12	Deformed rebar	120	120	3
MS55G16V12a	0.55	16	Plain bar	120	120	3
MS45G12V12a	0.45	12	Plain bar	120	120	3
MS35G12V12a	0.35	12	Plain bar	120	120	3

MS, mortar strength grade; G, plain bar; L, deformed bar; V, loading rate; a, anchorage length.
Numbers following MS, G(L) and V refer to w/c ratio, anchorage length and loading rate, respectively.

Table 2. Rank classification of strain rates and loading rates

Load types	Strain rate/s-1	Loading rate v/(mm·s-1)
Creep	$<10^{-6}$	$<10^{-2}$
Static state	10^{-6}~10^{-4}	10^{-2}~10^{0}
Seismic load (dynamic)	10^{-4}~10^{-2}	10^{0}~10^{2}
Impact load	10^{-2}~10^{1}	10^{2}~10^{5}
Blast	$>10^{2}$	$>10^{5}$

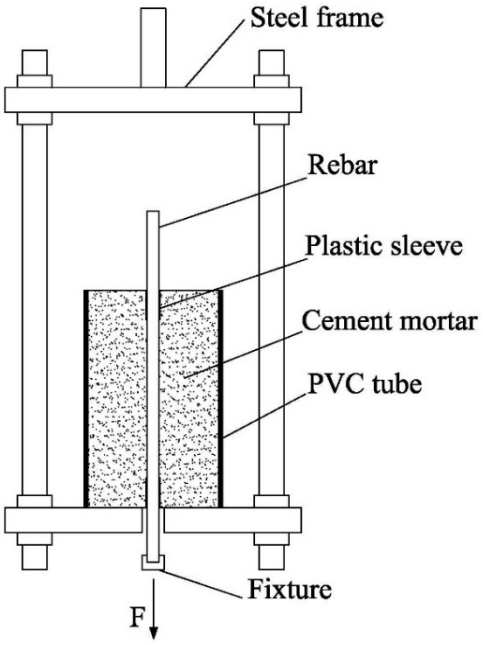

Figure (5): A schematic diagram showing loading setup

Test Results

Fig. 6 shows the strain curve of the steel bar obtained by the typical specimens, where *x* is the distance between the strain gauges and the load end. With the increase of the load, the strain of the steel bar increased gradually along the anchoring. However, due to the bond stress between the mortar and the steel bar, where the bond stress offset partial tension is transmitted along the anchoring depth, the strain decreased gradually with the same load.

According to *x*=0mm (the loading end) in the load-strain curve, the curve changed linearly, where the slope was approximately equal to *EsAs*, indicating that the steel bar was in a purely tensile state and the bond stress was generated from this point. For the measuring points away from the loading end, the strain increased slowly with the increasing pull-out load where the larger the anchoring depth, the slower the strain growth. This phenomenon can be explained by the following reasons. When the load was small, the bond stress played the major role. When the free end started slipping with the increasing load, the strain of the steel bar increased and the bond between the steel bar and the mortar was broken.

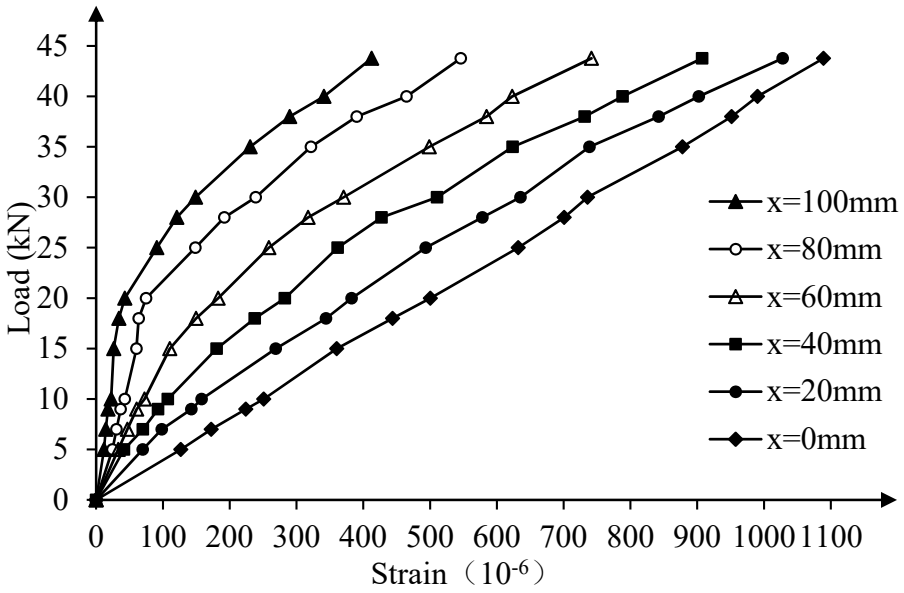

Figure (6): Load-strain curve for steel reinforcement at different points along the anchor length of specimen MS55G16V8a

The strain of the steel bar varied with the load and the loading rates along the anchoring depth are shown in Figs. (7-9). According to the analysis of the curve, it can be seen that as the pull-out load transferring along the anchoring depth was impeded by the bond stress in the anchorage body during the pull-out process, the strain of the steel bar gradually decreased along the anchoring depth. Meanwhile, the smaller the load was, the smaller was the change rate of strain. With the load increasing gradually, the strain of the steel bar and the bond stress increased gradually and the peak of the bond stress translated towards the free end. The higher the loading rate was, the faster and more notably the strain varied. As the loading rate increased, the rising part of the bond stress curve was steeper and the peak value of the curve was larger. With high loading rate, the distance between the bond stress peak and the loading end was short due to bond damage and bond deterioration near the loading end.

Analysis of Influencing Factors

Loading Rate

With the diameter of 16 mm, the anchor length of 120 mm and the water-cement ratio of 0.55, the specimens were tested at the loading rates of 60

mm/min(1mm/s), 80 mm/min, 100 mm/min and 120 mm/min (2mm/s), respectively, to study the effect of loading rate on the bond performance. With the load F of 15 kN F_{max}（breaking moment）, the variations of strain and stress are shown in Fig. 10 (a) and Fig. 10 (b), respectively.

Fig. 10 (a) shows that as the loading rate increased, the strain of the steel bar decreased faster in the anchoring depth. At the breaking moment, however, the strain of the specimen with higher loading rate was larger. In order to better study the influence of the loading rate on the bond performance, the bond stress along the anchoring depth was plotted in Fig. 10 (b). Under the same load, due to the bond degradation and partial bond damage, the curve peak of the bond stress was larger and the rising part became steeper with the increase of the loading rate. The size of the area formed by the instantaneous bonding stress curve and the X axis is the strength of the bonding performance. It can be seen from the figure that when the loading rate was higher, the bond performance was better and the curve peak was closer to the loading end.

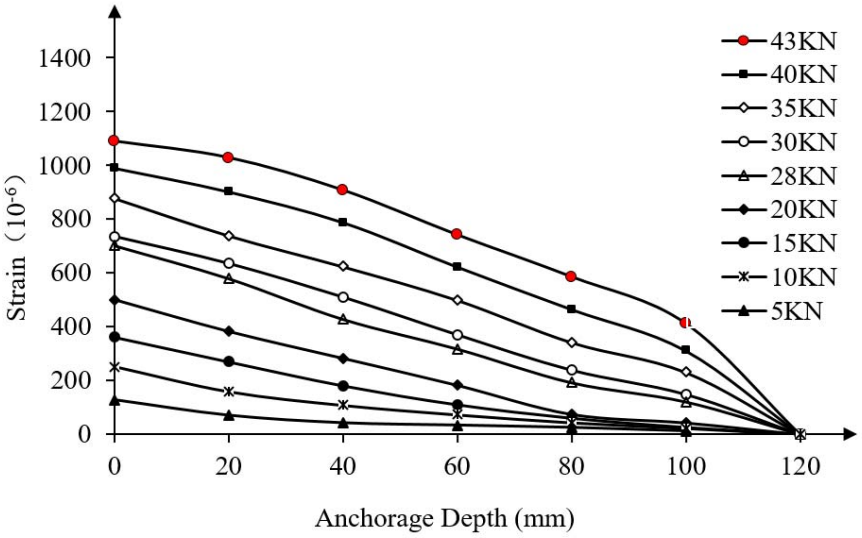

Figure (7): Strain in reinforcement of specimen MS55G16V8a under varying pull-out loads

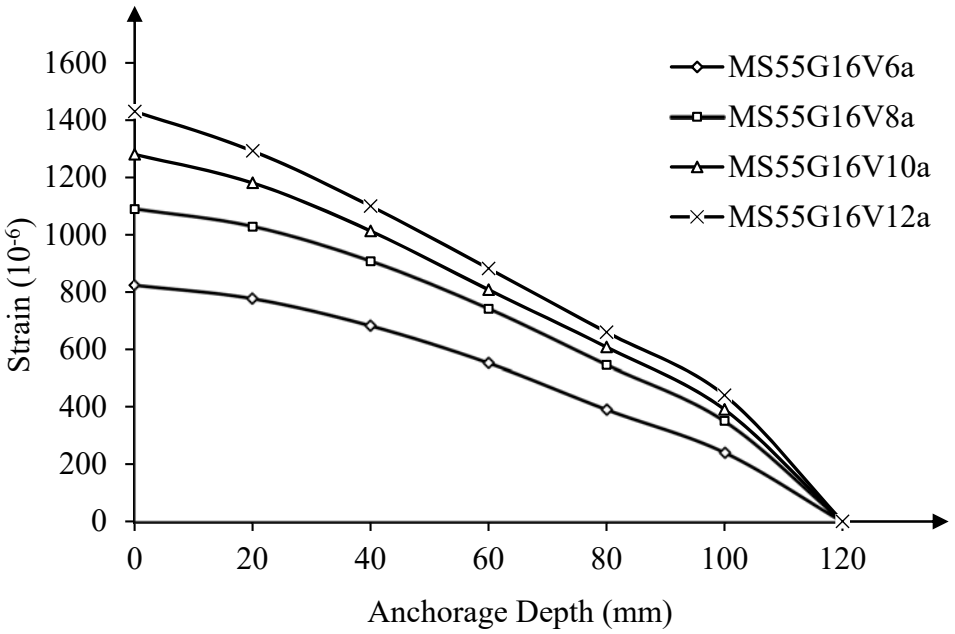

Figure (8): Strain in reinforcement of similar specimens subjected to different loading rates

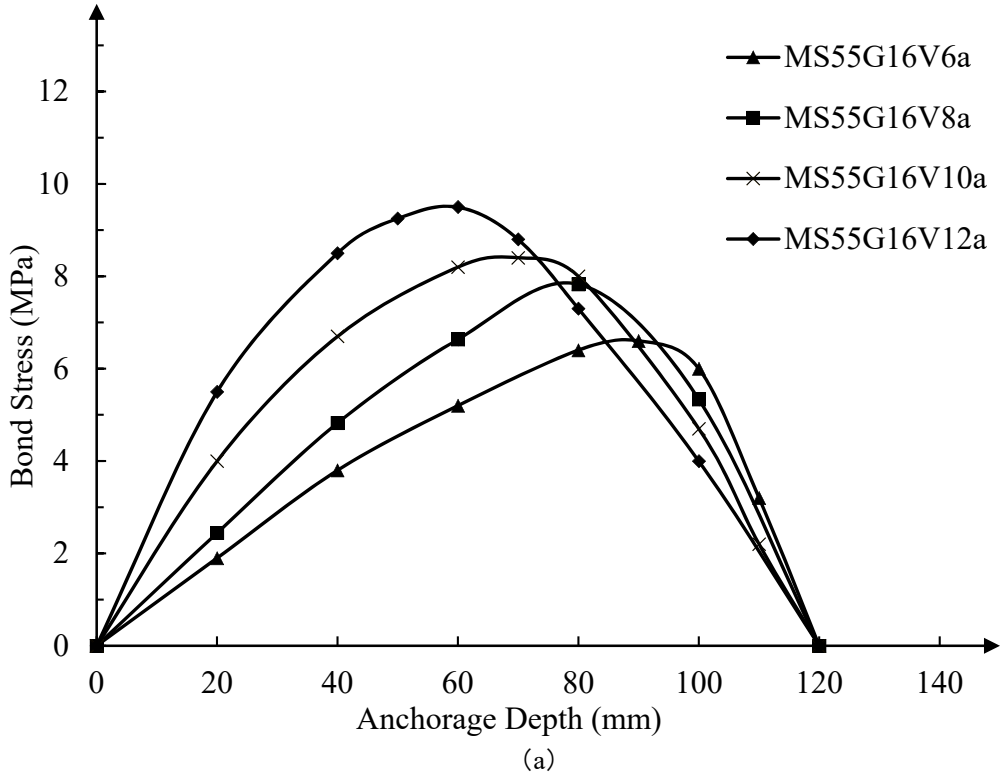

(a)

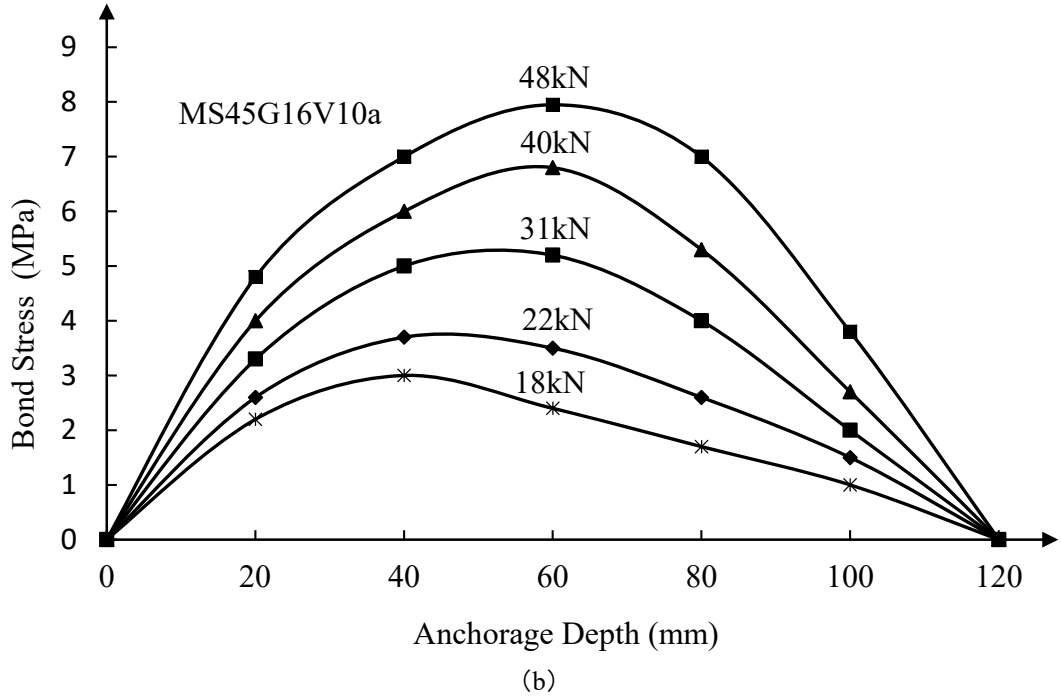

(b)

Figure (9): Bond stress along the anchorage depth for different specimens under different pull-out loads

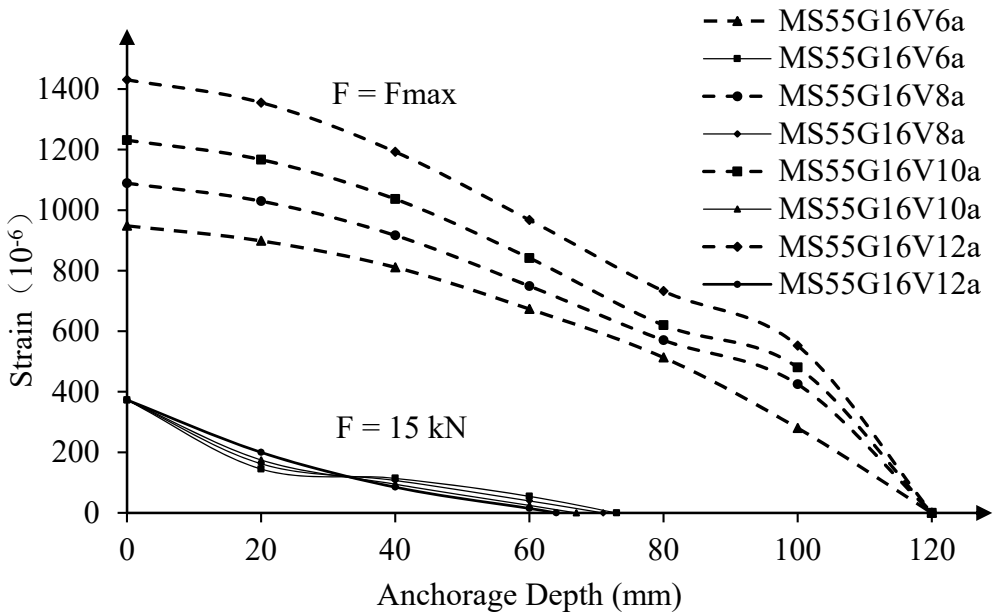

(a)

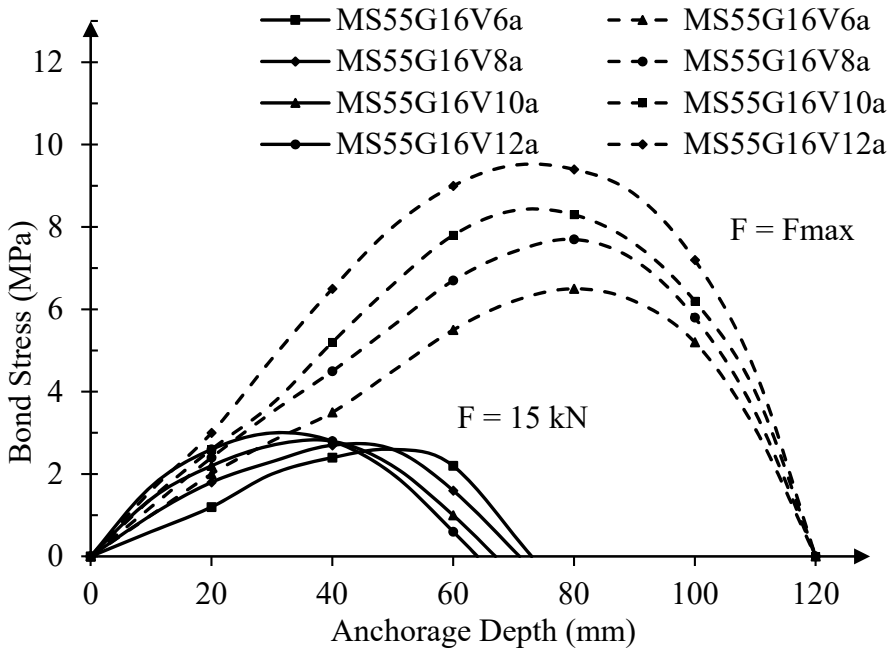

（b）

Figure (10): Influence of loading rate and level on the performance of bond stress-anchorage depth

Anchoring Length

Several specimens with different anchoring lengths were designed to study the influence of anchoring length on the bond performance. The average bond stress was used to reflect the bond performance of mortar anchors with different anchoring lengths. According to the experimental data, the average bond stresses at different anchoring lengths and different loading rates were obtained, as presented in Fig. 8, where the average bond stress is the average value measured for several specimens with the same parameters.

Fig. 11 shows that at the same loading rate, the average bond stress of the mortar anchor gradually decreased with the increase of the anchoring length.

However, the sum of the bond stresses at each point in the anchorage section increased gradually and the ultimate bearing capacity of pull-out load increased. Compared with the situation under static load, the bond performance between the steel bar and the mortar improved greatly under dynamic load.

Mortar Strength

Specimens with different mortar strengths were tested for the study of the influence of mortar strength on the bonding properties. When the other parameters were kept constant, specimen MS35G12V10a with the mortar strength of 55.1MPa, specimen MS45G12V10a with the mortar strength of 43.5MPa and specimen MS55G12V10a with the mortar strength of 32.7Mpa were used for analysis. The variations of strain steel bar and bond stress along the anchoring depth of each mortar strength are presented in Fig. 12 and Fig. 13, respectively.

Fig. 12 shows the variation of strain of the steel bar at each measuring point along the anchoring depth at the moment of failure. It can be seen from the figure that the strain of the steel bar increased gradually with the increase of the mortar strength. Along the anchoring depth, the greater the mortar strength, the higher the change rate of the strain. Fig. 13 shows the variation of the bond stress along the anchoring depth under different loads. It can be seen that the curve peak of the bond stress was close to the loading end when the load was small, but the distance that the bond stress transmitted along the anchoring depth was short. Under the critical state (breakdown point), the maximum bond stress increased with the increase of the mortar strength and the bond performance between the steel bar and the mortar was enhanced.

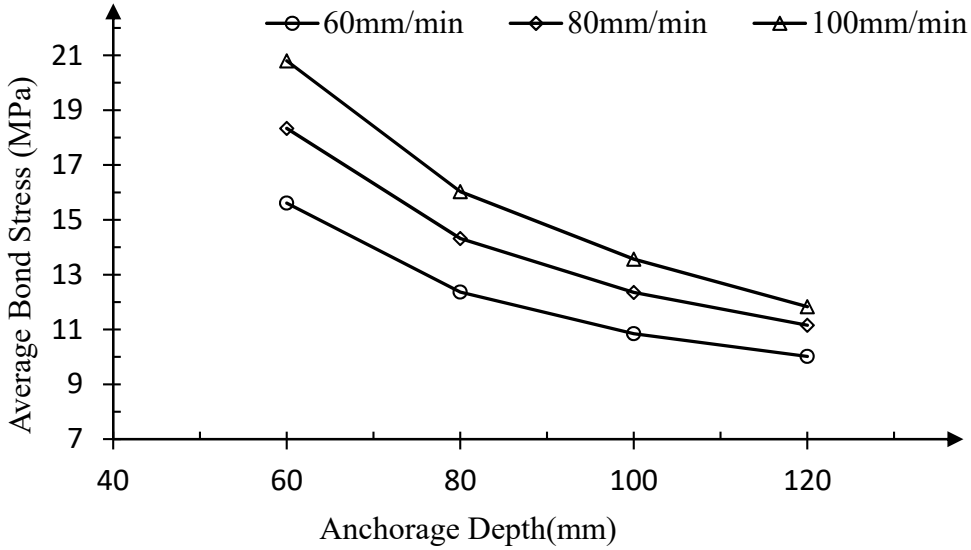

Figure (11): Average bond stress curves for different anchorage lengths

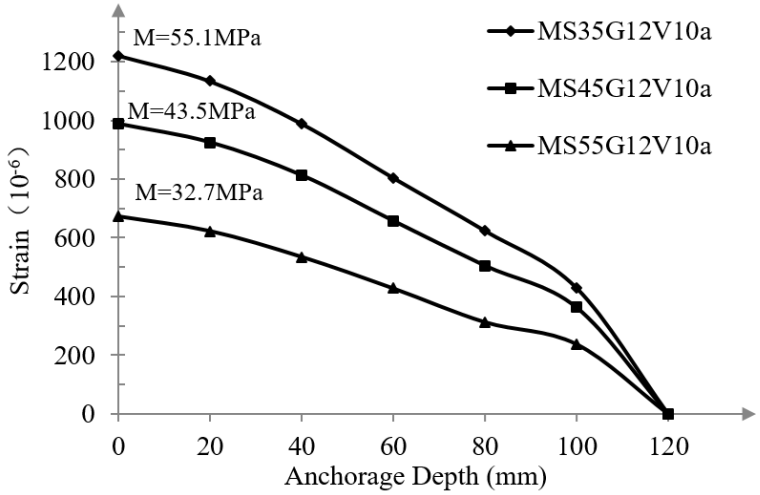

Figure (12): Strain distribution along anchorage length considering different mortar strengths

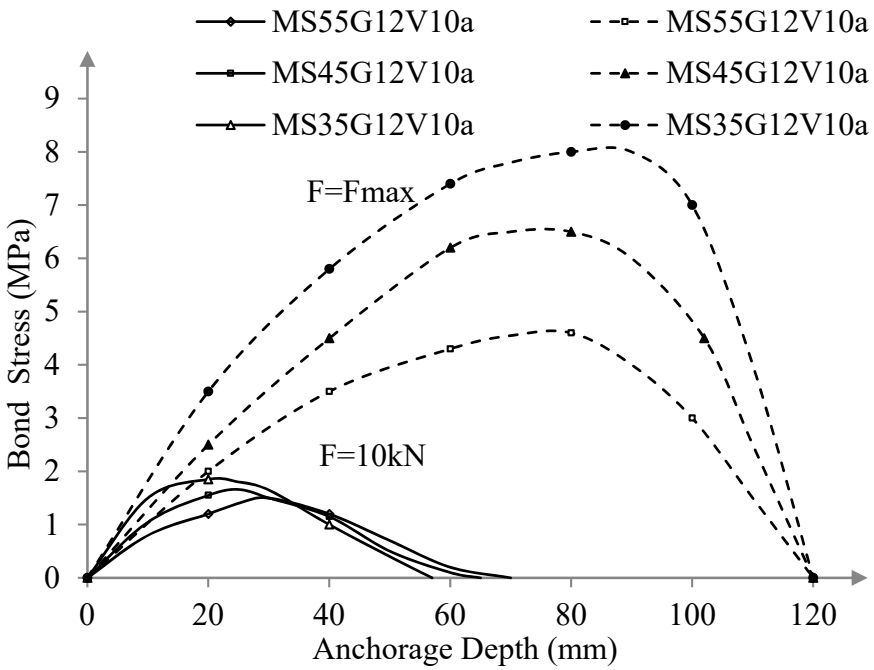

Figure (13): Stress distribution along anchorage length considering different mortar strengths

CONCLUSIONS

The bond properties of the mortar anchor at different loading rates were investigated by the dynamic pull-out test. The variations of the strain of the steel bar and the bond stress were analyzed. The parameters affecting the bond performance between the steel bar and mortar were also studied. The following conclusions have been drawn:

With the increase of the loading rate, the strain of the steel bar along the anchoring depth gradually decreased and the decreasing rate increased gradually. Due to bond degradation and partial bond damage, under the same load, the increasing loading rate also resulted in an increasing curve peak of the bond stress and steeper rising part. Meanwhile, the distance that the bond stress transmitted along the anchoring depth was shorter. As the load increased during the pull-out process, the peak value of the bond stress translated to the deeper anchorage section. The specimens with large loading rate had greater peak value of the bond stress and their bond performance was good.

With the increase of the anchorage length of the steel bar, the ultimate bearing capacity of the pull-out load increased gradually. The average bond stress calculated according to the ultimate bearing capacity decreased gradually. However, the sum of bond stresses at each point in the anchorage section gradually increased and the bond performance was gradually enhanced.

With the increase of the mortar strength, the strain of each measuring point in the anchorage section increased gradually during the pull-out test and the change rate of strain along the anchoring depth was larger. Under the same load level, the bond performance was improved with the increase of the mortar strength. Meanwhile, with high mortar strength, the curve peak of the bond stress was closer to the loading end and the distance that the bond stress transmitted along the anchoring depth was short. Under the critical state, the maximum bond stress increased gradually and the bond performance gradually increased.

Funds:
Ministry of Science and Technology of China (2018M631330)
Foundation for University Innovative Talents for Liaoning Province of China (LR2017047)
Foundation for Dalian Distinguished Young Scholars (2018RJ10).

REFERENCES

Ahmet Teymen. (2017). "Effect of mineral admixture types on the grout strength of fully-grouted rock bolts". Construction and Building Materials, 145, 376-382.

Ankur Tailor, Sejal Dalal, and P.D. Dalal. (2017). "Comparative performance evaluation of steel column building and concrete filled tube column building under static and dynamic loading". Jordan Journal of Civil Engineering, 11 (2).

Anwar, A., Alnaki, Falah M. Wegian, Magdy A. Abdalghaffar, Fahad A. Alotaibi, Abdul-Salam A. Al-Temeemi, and Mohammad T. Alkhamis. (2013). "Behavior of high-performance pull-out bond strength of fiber-reinforced concrete structures". Jordan Journal of Civil Engineering, 7 (1).

Caliskan, S., and Karihaloo, B.L. (2004). "Effect of surface roughness, type and size of model aggregates on the bond strength of aggregate-mortar interface". Interface Science, 12, 361-374.

Chen, W., Lu, F., and Cheng, M. (2002). "Tension and compression tests of two polymers under quasi-static and dynamic loading". Polymer Testing, 21, 113-121.

Farmer, I.W. (1975). "Stress distribution along a resin-grouted rock anchor". International Journal of Rock Mechanics, Mining Sciences & Geomechanics Abstracts, 12 (11), 347-351.

Flavio de Andrade Silva, Marko Butler, Viktor Mechtcherine, Deju Zhub, and Barzin Mobasherb. (2011). "Strain rate effect on the tensile behaviour of textile-reinforced concrete under static and dynamic loading". Materials Science and Engineering, A, 528, 1727-1734.

Gang Wang, Xuezhen Wu, Yujing Jiang, Na Huang, and Shugang Wang. (2013). "Quasi-static laboratory testing of a new rock bolt for energy-absorbing applications". Tunnelling and Underground Space Technology, 38, 122-128.

Hanson, N.W. (1969). "Influence of surface roughness of pre-stressing strand on bond performance". Journal of Pre-stressed Concrete Institute, 14 (1), 32-45.

Jeng, F.S., and Huang, T.H. (1999). "The holding mechanism of under-reamed rock bolts in soft rock". Int. J. Rock Mech. & Min. Sci., 36, 761-775.

Louis, N.S., Chiu, Brian G. Falzon, Dong Ruan, Shanqing Xu, Rodney S. Thomson, Bernard Chen, and Wenyi Yan (2015). "Crush responses of composite cylinder under quasi-static and dynamic loading". Composite Structures, 131, 90-98.

Lutz, L., and Gergeley, P. (1967). "Mechanics of band and slip of deformed bars in concrete". Journal of American Concrete Institute, 64 (11), 711-721.

Pabitra Rajbongshi, Mitali Saharia, Kh., and Lakshman Singh. (2019). "Stress characterization in visco-elastic asphalt mixes under different dynamic loadings". Jordan Journal of Civil Engineering, 13 (4).

Sreedhar Kalavagunta, Sivakumar Naganathan, Kamal Nasharuddin Bin Mustapha, and Ahmad Shabir Rezaii. (2016). "Experimental investigation of bond characteristics between CFRP and steel under tensile loads". Jordan Journal of Civil Engineering, 10 (3).

Tassios, T.P., and Yannopoulos, P.J. (1981). "Analytical studies on reinforced concrete members under cyclic loading based on bond stress-slip relationships". ACI Journal, 78 (3), 206-216.

Wang Hai-tao, Shen Jiayu, Wu Feng, An Zhiqiang, and Liu Tianyun. (2019). "Experimental study on elastic-plastic seismic response analysis of concrete gravity dam with strain rate effect". Soil Dynamics and Earthquake Engineering, 116 (1), 563-569.